Communication in Physical Sciences, 2024, 12(1): 026-037

Resource recovery from Sugar Cane Biomass for the Synthesis of Silicon Nanoparticles

Irene Edem Johncross, Abidemi Obatoyinbo Ajayi and Abidemi Obatoyinbo Ajayi
Received: 19th May 2024/Accepted: 09 November 2024/First Published: 14 November 2024, doi: https://dx.doi.org/10.4314/cps.v12i1.4

Abstract: *This study presents a green synthesis approach for silicon oxide nanoparticles (SiONPs) using plantain peels, highlighting their structural and surface properties, potential applications, and environmental benefits. UV-visible absorption spectroscopy revealed a peak absorption at 341 nm, corresponding to a bandgap of 3.87 eV, confirming the semiconductor nature of the synthesized SiONPs. The X-ray diffraction (XRD) analysis displayed a prominent peak at 69.24°, indicative of high crystallinity and minimal amorphous content, with a calculated crystallite size of 0.23 nm based on Scherrer's equation. Brunauer-Emmett-Teller (BET) surface area analysis showed a surface area of 198.98 m²/g, exceeding literature values and suggesting enhanced adsorption properties. Additional analyses using Barrett-Joyner-Halenda (BJH), Dubinin-Radushkevich (DR), and Density Functional Theory (DFT) models indicated a mesoporous structure with an average pore diameter of 5.5545 nm and a pore volume of 0.0371 cc/g, suitable for applications requiring high surface area-to-volume ratios. Compared to reported values for SiONPs synthesized by traditional methods, the SiONPs obtained from plantain peel demonstrate promising structural integrity and mesoporosity. This research emphasizes the feasibility of using agro-waste for nanoparticle synthesis, offering a sustainable alternative with potential applications in environmental remediation and catalytic processes.*

Keywords: *Resource recovery, sugar cane wastes, silicon nanoparticles, synthesis, characterization.*

Irene Edem Johncross
Department of Chemistry, National Open University of Nigeria, Jabi, Abuja, Nigeria
Email: irene.johncross@gmail.com
Orcid id: 0009-0009-1894-7239

Fanifosi Seyi Josiah
Klipsch School of Electrical and Computer Engineering, New Mexico State University, USA.
Email: seyifanifosi@yahoo.com

Abidemi Obatoyinbo Ajayi
Department of Mechanical and Aerospace Engineering, College of EngineeringNew Mexico State University, Las Cruces, USA.
Email: demijay@nmsu.edu

1.0 Introduction

In recent years, nanotechnology has seen remarkable advancements, particularly in the development and application of nanoparticles, which have revolutionized fields as diverse as electronics, catalysis, environmental science, agriculture, biomedicine, and energy storage. Nanoparticles, characterized by diameters between 1 and 100 nm, exhibit unique structural properties that enable their classification into microporous (0-2 nm), mesoporous (2-50 nm), and macroporous (50-100 nm) categories, depending on their specific pore sizes (Eddy et al., 2021, 2022a,b); 2023a-c; Weisany, *et al*., 2024). This fine structural tuning grants nanoparticles exceptional versatility and functionality, which make them highly suited for applications like drug delivery systems, sensors, and nanocomposites.

Among these nanoparticles, silicon oxide (SiO_2) nanoparticles have gained significant interest due to their distinctive attributes, including a high surface-to-volume ratio,

porosity, excellent adsorption properties, stability, biocompatibility, and adaptable surface chemistry (Rastogi, *et* al., 2024; Vasilyeva *et al*., 2024). These characteristics facilitate their integration with various functional molecules, broadening their applications across numerous industries such as construction (refractory materials, high-performance cement), coatings, agriculture (bio-fertilizers), and even cosmetics (Ghorbani *et al*., 2015; Kim and Lee, 2023; Yan *et al*., 2024). Silicon dioxide, or silica, also stands out as a naturally abundant mineral, primarily found as amorphous silica in plant biomass (Anuar et al., 2018; Saha *et al*., 2024).

Traditional methods for synthesizing silica nanoparticles—such as sol-gel processes, thermal decomposition, and high-temperature reactions—often rely on hazardous chemicals, consume considerable energy, and produce environmentally detrimental by-products like sodium sulfate and carbon dioxide (Elizondo-Villarreal *et* al., 2024; Khatoon *et al*., 2024; Mahawar *et al*., 2023). In response to these environmental concerns, research has increasingly focused on biosynthetic approaches that utilize renewable resources, including agricultural waste, as green alternatives. Agricultural residues such as rice husks, plantain peels, and sugar cane bagasse, which are typically discarded, have shown promising potential as sources for silica extraction, offering advantages in cost-efficiency, abundance, and environmental sustainability (Shanmugavadivu et al., 2014; Corrales-Urea et al., 2020).

This study seeks to harness the potential of sugar cane waste for synthesizing silicon oxide nanoparticles, a process that aligns with sustainable waste management and the shift towards green synthesis in nanotechnology. By transforming agricultural waste into valuable nanomaterials, this research contributes to both waste reduction and the provision of eco-friendly raw materials for high-demand applications.

2.0 Materials and Methods

2.1 Materials

Sugar cane biomass was collected as waste from local sugar cane vendors. Sulfuric acid (H_2SO_4), sodium hydroxide (NaOH), and other chemicals used in this study were of analytical grade, purchased from a reputable supplier, and used without further purification. Distilled water was used for washing and dilution throughout the study.

2.2 Preparation of Sugar Cane Biomass

The collected sugar cane biomass was thoroughly washed with distilled water to remove any adhering dirt and impurities. The washed biomass was then air-dried for 24 hours, followed by drying in an oven at 60°C for 6 hours to remove moisture content. The dried biomass was subsequently ground into a fine powder using a mechanical grinder and sieved to obtain a uniform particle size.

2.3 Extraction of Silicon from Sugar Cane Biomass

The powdered sugar cane biomass was subjected to acid leaching to remove unwanted impurities. The biomass was treated with 2 M sulfuric acid (H_2SO_4) and stirred for 2 hours at 80°C. The acid-treated sample was filtered and rinsed thoroughly with distilled water until a neutral pH was achieved. After drying, the sample was subjected to calcination at 650°C for 4 hours to produce a high-purity silica (SiO_2) precursor.

2.4 Synthesis of Silicon Oxide Nanoparticles (SiONPs)

The silica precursor obtained from the calcined sugar cane biomass was further processed to synthesize silicon oxide nanoparticles. A solution of 1 M sodium hydroxide (NaOH) was prepared, and the calcined silica was added to it, followed by stirring at 90°C for 3 hours to form a sodium silicate solution. This solution was filtered and then titrated with 1 M sulfuric acid (H_2SO_4) to precipitate silicon oxide nanoparticles. The precipitate was collected,

washed, and dried at 100°C for 6 hours to obtain pure silicon oxide nanoparticles.

2.5 Characterization of Silicon Oxide Nanoparticles

The UV-visible absorption spectra of the silicon oxide nanoparticles were recorded using a UV-visible spectrophotometer over a wavelength range of 200–800 nm. The sample was dispersed in distilled water and sonicated for 10 minutes to ensure uniform particle suspension. This analysis allowed for the determination of the optical properties, including the maximum absorbance (λ_max) and optical band gap.

BET analysis was performed to determine the specific surface area, pore volume, and pore size distribution of the silicon oxide nanoparticles. Before the analysis, the sample was degassed at 150°C under vacuum to remove any adsorbed contaminants. Nitrogen gas was used as the adsorbate, and the BET surface area was calculated from the nitrogen adsorption-desorption isotherms. Pore size distribution and pore volume were also evaluated based on the isotherm data, providing insights into the porosity and adsorption properties of the synthesized nanoparticles.

XRD analysis was conducted to determine the crystalline structure and phase purity of the synthesized silicon oxide nanoparticles. The powdered sample was scanned using an X-ray diffractometer with Cu-Kα radiation (λ = 1.5406 Å) over a 2θ range of 10–80°. The diffractogram obtained was used to calculate the crystallite size using the Debye-Scherrer equation. Additionally, the analysis provided information on the phase and crystallinity of the silicon oxide nanoparticles.

3.0 Results and Discussion

3.1 Absorption Spectrum

The UV visible absorption spectrum of the silicon oxide nanoparticles (SiONPs) synthesized from plantain peel is shown in Fig.1. The spectrum reveals maximum absorption within the ultraviolet region, which corresponds to the peak value of 341 nm. The observed absorption maxima for the SiONPs are in agreement with the ranges of values reported in literature values such as 259 nm (Saravanan and Dubey, 2020; Nimah *et al*., 2023). Also, a λ_{max} of 297 nm has also been reported by Biradar *et al*. (2021) for SiONPs and 485 nm by Intartaglia *et al*. (2012).

The wavelength of maximum absorption is a significant parameter in identifying a compound and in the calculation of the band gap of the nanomaterial. The calculation of the bandgap can be achieved through Planck's or Tauc's equations. For the synthesized SiONPs, the bandgap was evaluated using Planck's equation represented by equation1 (Ogoko *et al*., 2023)

$$E_{BG} = \frac{hc}{\lambda_{max}} \quad (1)$$

where h is the Planck constant and c is the speed of light. The insertion of the numerical constants and λ_{max} Equation 4.1 led to a value of 3.87 eV as the E_{BG}. The observed band gap shows some significant improvement over some literature values such as 7.4 eV (Cañas *et* al., 2024) but shows some agreement with the value of 3.6 eV reported by Guler *et al*. (2020) and Hussin *et al*. (2016). Also, a λ_{max} of 235 nm has been reported for silicon oxide nanoparticles synthesized by the sol gel method by Hussin, *et al*. (2016). The evaluated λ_{max} suggest that the synthesized SiONPs is a semiconductors.

2.2 XRD analysis

The XRD spectrum of silicon oxide nanoparticles is shown in Fig. 2. The spectrum reveals an almost single peak at 69.24 ° while insignificant peaks were obtained at 47.84 and 40.24 °. The prominent peak at 69 ° is due to Si(100) or Si (400). The observed peak portrays a high degree of crystallinity with an almost zero amorphous character. Several peak locations have been observed for SiONPS. Daulay *et al*. (2022) observed absorption peaks at 28.38, 47.26, 56.08, and 69.08° for SiONPs,

etc. The observation of less noise also confirmed the crystallinity of the synthesized SiONPs (Odoemelam *et al*., 2023). The crystallite size of the orange peel-based SiONPs was evaluated using Scherrer's equation which can be written according to equation 4.1 (Eddy *et al*., 2023a-b),

$$\beta(\theta) = \frac{k\lambda}{Lcos\theta} \quad (2)$$

where θ is the angle of diffraction, k is the Scherrer's constant, (0.9) λ is the wavelength of the Cu-K X-ray ($\lambda = 1.5406\, nm$) and L is the full width at half maxima. The equation reveals that peak width due to crystalline size varies directly with the crystalline size and becomes broad as the crystalline size increases.

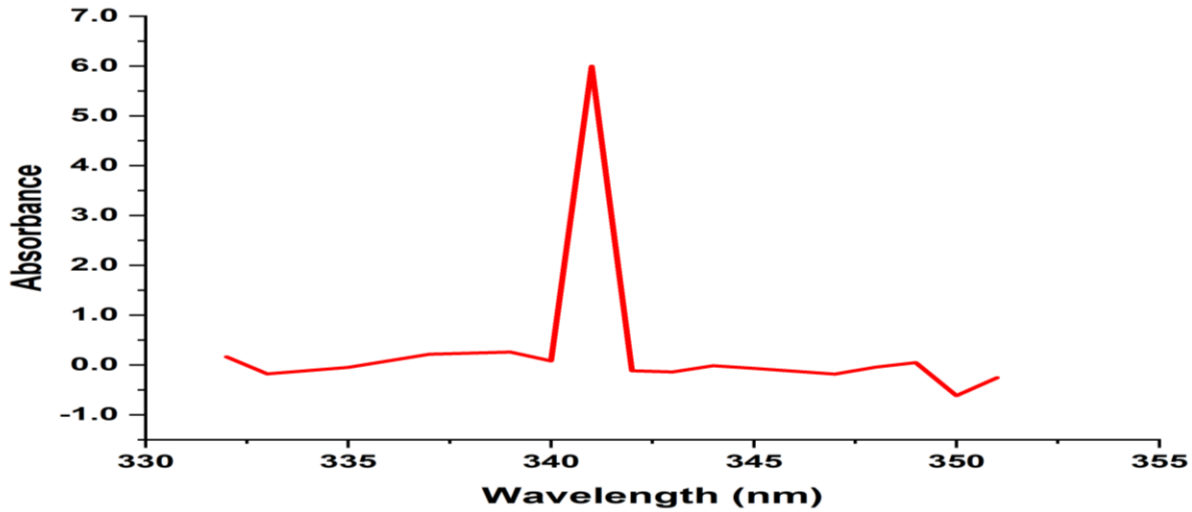

Fig. 1: UV visible absorption spectrum of SiONPs derived from plantain peels

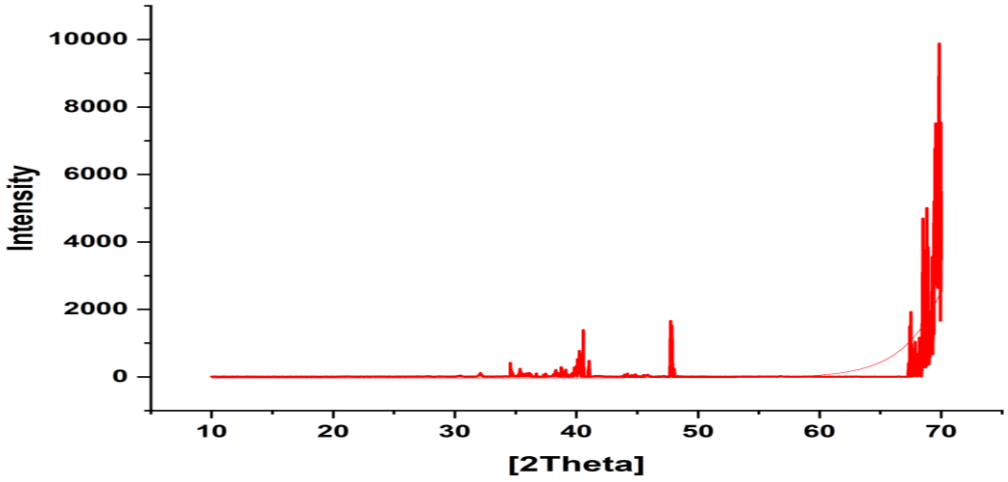

Fig. 2: XRD spectrum of SiONPs synthesized from orange peels

The origin software was used to evaluate the full width at half maximum through non-linear fitness of the peak function using the Gaussian function (with the model shown in Fig. 4.2) and the results obtained were $2\theta = 69.24$, L = 44.25, and R^2 = 0.9783, describing the fitness of the Gaussian curve with a standard error of 0.00123. The insertion of appropriate value into equation 4.2 indicated that the crystalline size of the CQDs is 0.23 nm. This value shows some merits in the expected performance of the SiONPs because the smaller the crystalline size, the better the efficiency of the SiONPs as nanoparticles (Yuan *et al*., 2018). The obtained

value for the crystallite size of the synthesized nanoparticles therefore shows some advantages over some literature values such as 20 nm (Abdul Ghani *et al*. 2017), 79 nm (Azib *et al*., 2021), 24.58 nm (Daulay *et al*., 2022)

2.3 BET surface analysis

The nitrogen absorption experiment was conducted to evaluate the pore volume, pore size and surface area of the nanoparticles through BET and DFT models. The Brunauer-Emmett-Teller (BET) properties of the nanoparticles were also investigated through the Multi-BET adsorption plot (which is based on equation 3) shown in Fig. 3 (Eddy *et* al., 2024a-c)

$$\frac{1}{X[(P_0/P)-1]} = \frac{1}{X_m} + \frac{C-1}{X_m C}\left(\frac{P}{P_0}\right) \qquad (3)$$

The fitness of the multi-BET model is accepted when a plot of values of $\frac{1}{X[(P_0/P)-1]}$ versus the relative pressure defined as $\left(\frac{P}{P_0}\right)$ is linear. Therefore, the slope and intercept should also be equal to $\frac{C-1}{X_m C}$ and $\frac{1}{X_m}$ respectively. In this model, X defines the amount of N_2 adsorbed at a pressure, P, X_m Represent monolayer adsorption capacity, P_0 is the initial pressure, and C is a constant that is proportional to the differences between the adsorption heat (q_{ads}) and the heat of condensation (q_{cond}) that is, $C = [q_{ads} - q_{cond}]/RT$.

From Fig. 3, the following values were obtained, namely, R^2 = 0.9766, slope = $\frac{C-1}{X_m C}$ = 13.9084 and intercept = $\frac{1}{X_m}$ = 3.5987. Hence the monolayer adsorption capacity defined as the inverse of the intercept is 0.27788 m^3. Also, from the value of the slope, the constant C was evaluated using the relation, $slope \times X_m = \frac{C-1}{C}$ and we obtained a numerical value of 4.5442, which means that $[q_{ads} - q_{cond}] = 0.2587\ J$. In a physical adsorption system, the value that expresses the differences between $q_{ads}\ and\ q_{cond}$ Represents the heat required to wet the surface before adsorption.

In this study, the approximate value of the heat required for surface wetting is evaluated as 3 268.96 kJ, which is only possible at a very high pressure. Also, the slope and intercept values were substituted to equation 4.4 to obtain the BET surface area (Eddy *et al*., 2022a).

$$Mult - BET\ (SA) = \frac{1}{\frac{1}{X_m} + \frac{C-1}{X_m C}} * A \qquad (4)$$

where A is the cross-sectional area. We obtained the numerical value of the surface area of the synthesized SiONPs as 198.98 m^2/g, which is higher than some literature values (Table 1). The Langmuir surface area was however observed to be equal to 626.81 m^2.

The pore volume and pore diameter of the nanoparticles was also evaluated using different isotherms including Barrett Joyner Halenda (BJH), Dubinin Raduskevich (DR) and the density functional theory model (DFT). The results obtained for the pore diameter, surface area, pore volume and surface area to volume ratio are recorded in Table 2 for the different models. The nanoparticles displayed a relatively large surface area to volume ratio, which is one of the major characteristics of nanoparticles (Eddy *et* al., 2024c). The average particle size was measured as 3.31 nm, which is acceptable for mesoporous materials because the pore diameter is within the range, 2 to 50 nm (Eddy *et al*.,2024d). Particle size, the porosity of nanoparticles can generally be classified into microporous (particle size less than 2 nm), mesoporous (particle size between 2 and 50 nm) and microporous (particle size between 50 and 100 nm) (Eddy *et al*., 2023c-d). However, the average pore volume was 0.0371 cc/g while the pore diameter was 5.5545 nm. Some reported values concerning the particle size of SiONPs are presented in Table 2. From the presented data, the synthesized SiONPs have particle sizes that are uniquely mesoporous. Some reported values of particles for SiONPs are 15 nm (Meng *et al*., 2020) and 27.77 nm (Daulay *et al*., 2022)

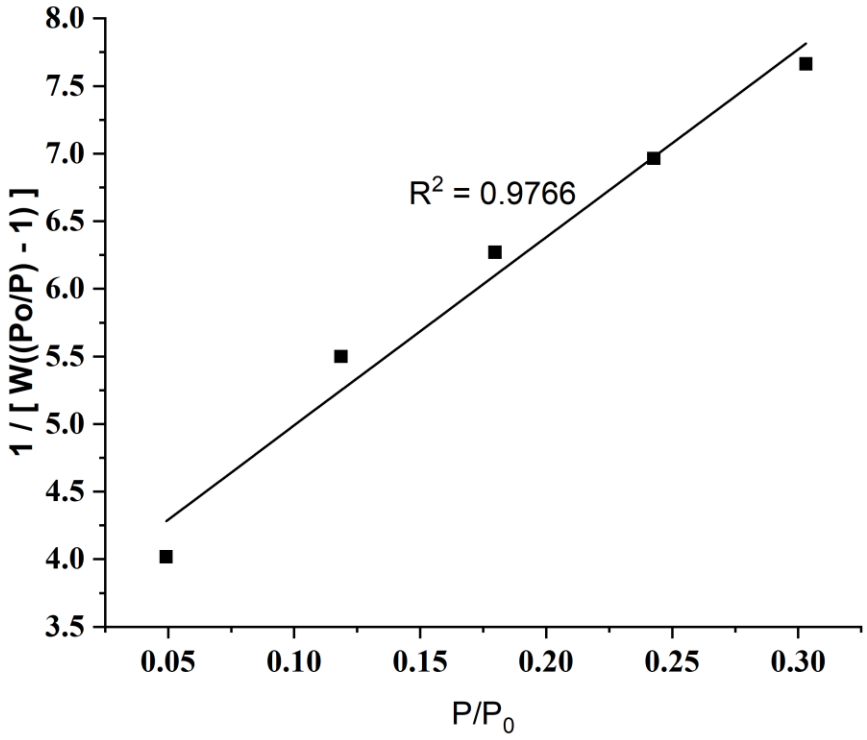

Fig. 3: Multi-Bet plot for SiONPs synthesized from sugar cane waste

Table 1: Pore Properties of the Synthesised CaO Nanoparticles

Model	Surface area (m^2/g)	Pore volume (cc/g)	Pore diameter (nm)	Surface area : volume
Multi-BET	198.90			
Langmuir	626.80			
BJH	247.10	0.1204	2.118	116.6667
DR	2228.20	0.0811	5.1670	431.2367
DFT	54.65	0.0648	2.6470	20.64601

Table 2: Literature Values of Source of Synthesis, Characterization and Surface Properties of SiONPs

Nanoparticles	Method	Synthetic condition	Characteristics	References
SiO-NPS	Sol gel method using $Si(OC_2H_5)_4$	650 °C, 4 hours, x = 58 nm,	FESEM, EDS	Chang *et al*. (2014),
SiO-NPS	Sol gel method using $Si(OC_2H_5)_4$	700 °C, 2 hours, x = 79.68 nm to 87.35 nm	FE-SEM, particle size analyser	Azlina *et al*I. (2016)

SiO-NPS	Sol gel method using $Si(OC_2H_5)_4$	500 °C, 1 hour, x = 193 nm, $x_{max} = 259\ nm$	UV-V, FTIR, DLS,	Saravanan and Dubey (2020)
SiO_2-NPS	Modified Sol gel method using HCl, NaOH and ashed plant wastes	650 °C, 2 hours, X = 193 , d = 53 nm, $x_{max} = 259\ nm$	FTIR, XRD,	Nimah *et al*. (2023)
SiO_2-NPS	Sequential method employing sonication to complete sol gel synthesis using $Si(OC_2H_5)_4$, NH_4OH as precursors	Calcination at 600 °C, 2 hours, x = 20 nm, d = 27 nm	UV-Vis, XRD, FTIR, TEM	Rao *et al*. (2005)
SiO_2-NPS	lyotropic liquid crystals formation method	x= 4 nm, SA = 587 m^2/g, PHZC = 3.1,	EDX, SEM, BET, PHZC	Arce et al. (2015)
SiO_2-NPS	Precipitation method using rice husk	650 °C , Purity = 95%, x = <100 nm	FESEM, XRF	Zarei *et al.* (2021)
SiO_2-NPS	Green synthesis using Rhus coriaria L. extract and sodium metasilicate	d =18 nm, x = 60 nm	XRD, TGA/DSC, FTIR, UV Vis, DLS	Rahimzadeh *et al*. (2022)
SiO_2-NPS	Facile approach	x = 67 nm	XRD, TEM, SEM, FTIR, TGA/DSC	Ismail *et al*. (2021)
SiO_2-NPS	Ultrasound-assisted sol-gel method using TEOS, NH_4OH and water	d = 28 nm, x = 48 nm, E_{BG} = 4.8 eV	SEM, TEM, XRD	Edriss and Adinehnia (2011)

4.0 Conclusion

This study successfully synthesized silicon oxide nanoparticles (SiONPs) from plant-based waste materials, specifically plantain peels, using green synthesis methods. The UV-visible absorption spectrum confirmed a maximum absorption peak at 341 nm, consistent with known values for silicon oxide nanoparticles, and a calculated bandgap of approximately 3.87 eV, suggesting that the synthesized SiONPs exhibit semiconductor properties suitable for applications in electronic and optoelectronic devices.

The XRD analysis revealed a prominent crystallinity peak at 69.24°, which aligns with the characteristic Si(100) or Si(400) crystallographic planes. The calculated crystallite size of 0.23 nm highlights the high degree of crystallinity and nanoscale structure of the SiONPs, offering advantages in potential catalytic and electronic applications. BET surface analysis determined a specific surface area of 198.98 m^2/g, while additional models, including Langmuir, Barrett-Joyner-Halenda (BJH), Dubinin-Radushkevich (DR), and Density Functional Theory (DFT), supported a

mesoporous structure with an average pore diameter of 5.55 nm, consistent with desirable properties for adsorption-based applications such as pollutant removal.

In view of the above findings and conclusion, the following recommendations are made,

(i) Given the high surface area and mesoporous nature of the synthesized SiONPs, their use as adsorbents for heavy metal and organic pollutant removal from wastewater should be explored. This could have significant implications for reducing pollution from industrial effluents.

(ii) Due to the bandgap energy observed, which positions the SiONPs as potential semiconductors, additional research into their photocatalytic behavior under UV and visible light could be beneficial. This could lead to applications in solar-driven photocatalysis for environmental cleanup and renewable energy generation.

(iii) The semiconductor characteristics and nanostructure suggest that SiONPs could be further investigated for electronic applications, including in the fabrication of sensors, energy storage devices, and other nanotechnology-based components.

(iv) Further studies on optimizing synthesis conditions for larger-scale production and evaluating the economic feasibility of the process using low-cost, locally available plant waste materials should be considered, especially within Nigeria and other regions where agricultural waste is abundant.

5.0 References

Abdul Ghani, N. A. M., Saeed, M. A. & Hashim, I. H. (2017). Thermoluminescence (TL) response of silica nanoparticles subjected to 50 Gy gamma irradiation.Maylaysian *Journal of Fundamental and Applied Sciences, 13, 3,* :doi:10.11113/mjfas.v13n3.593

Anuar, M.F., Fen, Y.W., Zaid, M.H.M., Matori, K.A., & Khaidir, R. (2018). Synthesis and structural properties of coconut husk as potential silica source. *Results in Physics, 11,* pp. 1-4. doi: 10.1016/j.rinp.2018.08.018018

Arce, J. V. R., Alburquenque, D., Gautier, J. L., Zuniga, G. A & Herrera, F. (2013). Simple steps for synthesis of silicon oxide mesoporous materials used as template. Journal of Chilean Chemical Society, 584, http://dx.doi.org/10.4067/S0717-97072013000400020

Azib, T., Thaury, C., Cuevas, F., Leroy, E., Jordy, C., Marx, N & Latroche, M. (2021). Impact of surface chemistry of silicon nanoparticles on the structural and electrochemical properties of $Si/Ni_{3.4}Sn_4$ composite anode for li-ion batteries. *Nanometerials (Basel), 11, 1,* doi: 10.3390/nano11010018

Azlina, H. N., Hasnidawani, J. N., Norita, H. & Surip, S. N. (2016). Synthesis of SiO2 Nanostructures Using Sol-Gel Method. *Acta Physica Polonica A, 29(*4): 842-844.

Biradar, A. I., Sarcalkar, P. D., Tell, S. R., Pawar, C. A., Patil, P. S. & Prasad, N. R. (2021). Photocatalytic degradation of dyes using one-step synthesized silica nanoparticles. *Materials Today Proceedings, 43, S1,* : doi:10.1016/j.matpr.2020.11.946.

Cañas, J., Reyes, D. F., Zakhtser, A., Dussarrat, C., Teramoto, T., Gutiérrez, M., & Gheeraert, E. (2022). High-quality SiO2/O-terminated diamond interface: Band-gap, band-offset, and interfacial chemistry. *Nanomaterials, 1, 23, pp.* , 4125. https://doi.org/10.3390/nano12234125

Chang, H., Kao, M. J., Hsu, F. C. & Peng, D. X. (2014). Synthesis and Characterization of SiO_2 Nanoparticles and Their Efficacy in Chemical Mechanical Polishing Steel

Substrate. Advances in Materials Science and Engineering, https://doi.org/10.1155/2014/691967.

Corrales-Ureña, Y., Villalobos-Bermudez, C., Pereira, R., Camacho, M., Estrada, E., & Argüello-Miranda, O. (2018). Biogenic silica-based microparticles obtained as a sub-product of the nanocellulose extraction process from pineapple peels. *Scientific Reports*, 8, pp. 1-9. doi: 10. -1038/s41598-018-28444-4s41598-018-28444-4Coti

Daulay, A., Andriayani., Marpongahtun & Gea, S. (2022). Synthesis Si nanoparticles from rice husk as material active electrode on secondary cell battery with X-Ray diffraction analysis. *South African Journal of Chemical Engineering*, 42: 32-41, https://doi.org/10.1016/j.sajce.2022.07.004.pp.

Eddy, N. O & Garg, R. (2021). CaO nanoparticles: Synthesis and application in water purification. Chapter 11. In: Handbook of research on green synthesis and applications of nanomaterials. Garg, R., Garg, R. and Eddy, N. O, edited. Published by IGI Global Publisher. DOI: 10.4018/978-1-7998-8936-6

Eddy, N. O., Garg, R., Garg, R., Aikoye, A. & Ita, B. I. (2022a). Waste to resource recovery: mesoporous adsorbent from orange peel for the removal of trypan blue dye from aqueous solution. *Biomass Conversion and Biorefinery*, DOI: 10.1007/s13399-022-02571-5.

Eddy, N. O., Garg, R., Garg, R., Eze, S. I., Ogoko, E. C., Kelle, H. I., Ukpe, R. A., Ogbodo, R. & Chijoke, F. (2023a). Sol-gel synthesis, computational chemistry, and applications of Cao nanoparticles for the remediation of methyl orange contaminated water. *Advances in Nano Research*, https://doi.org/10.12989/anr.2023.15.1.000

Eddy, N. O., Odiongenyi, A. O., Garg, R., Ukpe, R. A., Garg, R., El Nemir, A., Ngwu, C. M. & Okop, I. J. (2023b). Quantum and experimental investigation of the application of *Crassostrea gasar* (mangrove oyster) shell–based CaO nanoparticles as adsorbent and photocatalyst for the removal of procaine penicillin from aqueous solution. *Environmental Science and Pollution Research*, doi:10.1007/s11356-023-26868-8.

Eddy, N. O., Ukpe, R. A., Garg, R., Garg, R., Odiongenyi, A. O., Ameh, P., Akpet, I, N., & Udo, E. S. (2023c). Review of in-depth knowledge on the application of oxides nanoparticles and nanocomposites of Al, Si and Ca as photocatalyst and antimicrobial agents in the treatment of contaminants in water. Clean Technologies and Environmental Policy, DOI : 10.1007/s10098-023-02603-2.

Eddy, N. O., Jibrin, J. I., Ukpe, R. A., Odiongenyi, A., Iqbal, A., Kasiemobi, A. M., Oladele, J. O., & Runde, M. (2024b). Experimental and Theoretical Investigations of Photolytic and Photocatalysed Degradations of Crystal Violet Dye (CVD) in Water by oyster shells derived CaO nanoparticles (CaO-NP), *Journal of Hazardous Materials Advances*, 13, 100413, https://doi.org/10.1016/j.hazadv.2024.100413.

Eddy, N. O., Garg, R., Ukpe, R. A., Ameh, P. O., Gar, R., Musa, R., , Kwanchi, D., Wabaidur, S. M., Afta, S., Ogbodo, R., Aikoye, A. O., & Siddiqu, M. (2024c). Application of periwinkle shell for the synthesis of calcium oxide nanoparticles and in the remediation of Pb^{2+}-contaminated water. Biomass Conversion and Biorefinery, DOI: 10.1007/s13399-024-05285-y.

Eddy, N. O., Oladede, J., Eze, I. S., Garg, R., Garg, R., & Paktin, H. (2024a). Synthesis and characterization of CaO nanoparticles

from periwinkle shell for the treatment of tetracycline-contaminated water by adsorption and photocatalyzed degradation. *Results in Engineering*, *103374*. https://doi.org/10.1016/j.rineng.2024.103374.

Eddy, N. O., Garg, R., Garg, R., Garg, R., Ukpe, R. A. & Abugu, H. (2024). Adsorption and photodegradation of organic contaminants by silver nanoparticles: isotherms, kinetics, and computational analysis. *Environ Monit Assess*, 196, 65, https://doi.org/10.1007/s10661-023-12194-6.

Edriss, M. and Adinehnia, S. M. (2011). Synthesis of Silica Nanoparticles by Ultrasound-Assisted Sol-Gel Method: Optimized by Taguchi Robust Design. Chemical Engineering Technology, 34(11): 1813-1819, https://doi.org/10.1002/ceat.201100195.

Elizondo-Villarreal, N., Gandara-Martínez, E., García-Méndez, M., Gracia-Pinilla, M., Guzmán-Hernández, A. M., Castaño, V. M., & Gómez-Rodríguez, C. (2024). Synthesis and characterization of SiO_2 nanoparticles for application as nanoadsorbent to clean wastewater. *Coatings*, *14*, *7*, 919. https://doi.org/10.3390/coatings14070919

Ghorbani, F., Sanati, A. M., & Maleki, M. (2015). Production of silica nanoparticles from rice husk as agricultural waste by an environmentally friendly technique. *Environmental Studies of Persian Gulf*, 2, 1, pp. 56-65.

Hussin, S. H. A., Al-Hamdani, A. H. and Nazar, A. (2016). Optical and morphological characteristics for silicon dioxide NPS prepared by sol-gel method. International *Journal of Scientific and Engineering Research*, 7(8): 234-237.

Intartaglia, B., Bagga, K., Scotto, M., Diaspro, A. & Brandi, F. (2012). Luminescent silicon nanoparticles prepared by ultra short pulsed laser ablation in liquid for imaging applications. *Optical Materials*, 2, pp. 510-518

Ismail, A., Saputri, L. N. M. Z., Dwiatmoko, A. A., Susanto, B. H. and Nasikin, M. (2021) A facile approach to synthesis of silica nanoparticles from silica sand and their application as superhydrophobic material, *Journal of Asian Ceramic Societies*, 9, 2, pp. 665-672. doi: 10.1080/21 -870764.2021.1911057

Khatoon, N., Subedi, B., & Chrisey, D. B. (2024). Synthesis of silicon and germanium oxide nanostructures via photonic curing: A facile approach to scale up fabrication. *Chemistry Open, 13, 7,* e202300260. https://doi.org/10.1002/open.202300260.

Kim, T., & Lee, J. (2023). Silicon nanoparticles: Fabrication, characterization, application and perspectives. *Micro and Nano Systems Letters, 11, 18,* . https://doi.org/10.1186/s40486-023-00184-9.

Mahawar, L., Ramasamy, K. P., Suhel, M., Prasad, S. M., Živčák, M., Brestic, M., Rastogi, A., & Skalický, M. (2023). Silicon nanoparticles: Comprehensive review on biogenic synthesis and applications in agriculture. *Environmental Research*, *232*, 116292. https://doi.org/10.1016/j.envres.2023.116292.

Meng, T., Ying, K., Hong, Y. & Xu, Q. (2020). Effect of different particle sizes of nano-SiO_2 on the properties and microstructure of cement paste. *Nanotechnology Reviews*, https://doi.org/10.1515/ntrev-2020-0066

Ni'mah, Y. L. Muhainah, Z. H. & Suprapto, S. (2023). Synthesis of silica nanoparticles from sugarcane bagasse by sol-gel method. Nanoparticles, 4, 1, https://doi.org/10.35702/nano.10010.

Odoemelam, S. A., Oji, E. O., Eddy, N. O., Garg, R., Garg, R., Islam, S., Khan, M.

A., Khan, N. A. & Zahmatkesh, S. (2023). Zinc oxide nanoparticles adsorb emerging pollutants (glyphosate pesticide) from aqueous solution. *Environmental Monitoring and Assessment*, https://doi.org/10.1007/s10661-023-11255-0

Ogoko, E. C., Kelle, H. I., Akintola, O. & Eddy, N. O. (2023). Experimental and theoretical investigation of *Crassostrea* gigas (gigas) shells based CaO nanoparticles as a photocatalyst for the degradation of bromocresol green dye (BCGD) in an aqueous solution. *Biomass Conversion and Biorefinery*. https://doi.org/10.1007/s13399-023-03742-8

Rahimzadeh, C. Y., Barzinjy, A. A., Mohammed, A. S. and Hamad, S. M. (2022) Green synthesis of SiO_2 nanoparticles from Rhus coriaria L. extract: Comparison with chemically synthesized SiO_2 nanoparticles. *PLoS ONE* 17, 8, e0268184. https://doi.org/10.1371/journal.pone.0268184

Rao, K. S., El-Hami, K., Kodaki, T., Matsushige, K. & Makino, K. (2005). A novel method for synthesis of silica nanoparticles. *J Colloid Interface Sci*. 289, 11, pp. 125-31. doi: 10.1016/j.jcis.2005 - .02.019.

Rastogi, A., Tripathi, D. K., Yadav, S., Chauhan, D. K., Živčák, M., Ghorbanpour, M., El-Sheery, N. I., & Brestic, M. (2019). Application of silicon nanoparticles in agriculture. *3 Biotech, 9, 90*. https://doi.org/10.1007/s13205-019-1626-7.

Saha, A., Mishra, P., Biswas, G., & Bhakta, S. (2024). Greening the pathways: A comprehensive review of sustainable synthesis strategies for silica nanoparticles and their diverse applications. *RSC Advances, 14, pp.* 11197-11216. https://doi.org/10.1039/D4RA01047G.

Saravanan, S. & Dubey, R. S. (2020). Synthesis of SiO_2 nanoparticles by sol-gel method and their optical and structural properties. *Romanian Journal of Information Science and Technology*, 23, 1, pp. 105-112.

Vasilyeva, A. A., Buribaev, R. A., Gorbunova, M. V., Apyari, V. V., Torocheshnikova, I. I., & Dmitrienko, S. G. (2024). Silicon-based nanoparticles: Synthesis and recent applications in chemical sensing. *TrAC Trends in Analytical Chemistry, 171*, 117538. https://doi.org/10.1016/j.trac.2024.117538.

Weisany, W., Razmi, J., Hosseinzadeh Eshaghabadi, A., & Pashang, D. (2024). Silicon nanoparticles (SiNP): A novel and sustainable strategy for mitigating environmental stresses in plants. *Journal of Soil Science and Plant Nutrition, 24*, pp. 2167–2191.https://doi.org/10.1007/s42729-0 24-01790-1.

Zarei, V., Mirzaasadi, M., Davarpanah, A., Nasiri, A., Valizadeh, M. & Hosseini, M. J. S. (2021). Environmental method for synthesizing amorphous silica oxide nanoparticles from a natural material. *Processes*, 9, 334, https://doi.org/10.3390/ pr9020334.

Yan, G., Huang, Q., Zhao, S., Xu, Y., He, Y., Nikolic, M., Nikolic, N., Liang, Y., & Zhu, Z. (2024). Silicon nanoparticles in sustainable agriculture: Synthesis, absorption, and plant stress alleviation. *Frontiers in Plant Science, 15*. https://doi.org/10.3389/fpls.2024.1393458

Compliance with Ethical Standards Declaration

Ethical Approval

Not Applicable

Competing interests

The authors declare that they have no known competing financial interests

Funding

The work was supported by Prof. Nnabuk Okon Eddy, FAS trough the National Research Fund (Grant No: TRTF/ES/DR&D-CE/NRF2020/SETI/98/VOL.1)

Availability of data and materials

Data would be made available on request**.**

Author's Contribution

All authors contributed to the bench work and the writing of the manuscript.